

Theoretical and Experimental Study on Wave Damping inside a Rubble Mound Breakwater

M.O. Muttray ^{a,*}, H. Oumeraci ^b

^a*Delta Marine Consultants b.v., P.O. Box 268, 2800 AG Gouda, The Netherlands*

^b*Technical University Braunschweig, Leichtweiss Institute, Beethovenstr. 51a,
38106 Braunschweig, Germany*

Abstract

Wave decay in a rubble mound breakwater has been analysed theoretically for various types of damping functions (linear, quadratic and polynomial). The applicability of these damping functions for wave decay in the landward part of the breakwater core has been investigated in large scale model tests. The properties of the rock materials that has been used in the model tests have been determined to provide a rational basis for the damping coefficients. The analysis is based on detailed measurements of wave conditions and pressure distributions inside the breakwater. The theoretical approaches have been validated and where necessary extended by empirical means. The wave decay inside the breakwater can be reasonably approximated by the commonly applied linear damping model (resulting in exponential wave height attenuation). An extended polynomial approach provides a slightly better fit to the experimental results and reflects more clearly the governing physical processes inside the structure.

Key words: Rubble mound breakwater, wave damping, breakwater core

1 Introduction, previous work and methodology

The main purpose of rubble mound breakwaters is dissipation of wave energy. However a certain part of the incident wave energy will pass through the breakwater core resulting in wave disturbance at the lee side of the breakwater.

* Corresponding author

Email addresses: mmuttray@dmc.nl (M.O. Muttray), h.oumeraci@tu-bs.de (H. Oumeraci).

URLs: <http://www.dmc.nl>; <http://www.xbloc.com> (M.O. Muttray),
<http://www.lwi.tu-bs.de> (H. Oumeraci).

Wave transmission through a breakwater and wave damping inside a breakwater are highly complex processes. The porous flow inside a breakwater is turbulent, non-stationary and non-uniform. In the seaward part of the breakwater, two-phase flow (air–water mixture) is likely to occur.

The wave induced pore pressure distribution inside a breakwater is not or only to a minor extent considered in current design procedures. A revision of the actual design procedures has been proposed by several authors in the past decades (Bruun & Johannesson, 1976, for example). An improved breakwater design shall include a due consideration of the pore pressure distribution with respect to (i) slope failure analysis, (ii) optimised filter design and (iii) an improved prediction of wave transmission, wave run-up and wave overtopping as well as internal wave set-up (de Groot et al., 1994).

A relatively simple analytical method for the assessment of wave height attenuation inside a rubble mound breakwater is presented in this paper. The method has been derived theoretically and validated against experimental results from large scale model tests. The new method reflects the actual physical processes inside the breakwater more than existing approaches and proved to be more accurate.

1.1 Previous work: Hydraulic resistance

A number of serial and exponential approaches for the hydraulic resistance of coarse porous media have been developed for stationary flow (Hannoura & Barends, 1981). For non-stationary flow in coarse porous media the hydraulic resistance I can be approximated by the extended Forchheimer equation with an additional inertia term (Polubarinova–Kochina, 1962):

$$I = a v_f + b |v_f| v_f + c \frac{\partial v_f}{\partial t} \quad (1)$$

where a , b and c are dimensional coefficients and v_f is the flow velocity inside the porous medium (filter velocity). A set of widely used theoretical formulae for the Forchheimer coefficients a , b and c (see van Gent, 1992a) is presented in this section. Alternative approaches can be found in literature. Especially for coarse and wide graded rock material it might be necessary to determine the resistance coefficients experimentally.

Kozeny (1927) derived the coefficient a for stationary flow by considering the porous flow as capillary flow and the porous medium as a matrix of spherical

particles of equal size:

$$a = K_a \frac{(1-n)^2}{n^3} \frac{\nu}{gd^2} \quad (2)$$

with porosity n , grain size d , non-dimensional coefficient K_a and kinematic viscosity ν . Equation 2 has been confirmed theoretically and experimentally by Carman (1937), Ergun & Orning (1949), Ergun (1952), Koenders (1985), den Adel (1987), Shih (1990), van Gent (1992a) and by Burcharth & Andersen (1995). Various coefficients K_a that have been derived by these authors are listed in table 1. The large variability of the coefficient K_a should be noted.

The following approach for the resistance coefficient b , which includes the non-dimensional coefficient K_b (see table 1), has been proposed by Ergun & Orning (1949), Ergun (1952), Engelund (1953), Shih (1990), van Gent (1992a) and Burcharth & Andersen (1995) for stationary flow:

$$b = K_b \kappa_o \frac{1-n}{n^3} \frac{1}{gd} \quad (3)$$

The coefficient κ_o is 1 for stationary flow. If coefficient b accounts for viscous and turbulent shear stresses the Forchheimer equation will be applicable not only for combined laminar–turbulent flow, but also for fully turbulent flow (van Gent, 1992a).

The hydraulic resistance of a uniform non-stationary flow is described by the extended Forchheimer equation (equation 1). For oscillatory flow the additional resistance with regard to the convective acceleration has to be considered by a quadratic resistance term (Burcharth & Andersen, 1995). Hence, the resistance coefficient b will be increased. Van Gent (1993) determined experimentally a coefficient κ_o of $1 + 7.5/KC$ for oscillatory flow. The Keulegan–Carpenter number $KC = \tilde{v}_f T / (nd)$ characterises the flow pattern (with velocity amplitude \tilde{v}_f and period T) and the porous medium (particle size n and diameter d). The inertia coefficient c will not be affected by the convective acceleration and reads:

$$c = \frac{1}{ng} \left(1 + K_M \frac{1-n}{n} \right) \quad (4)$$

This approach has been used by Sollit & Cross (1972), Hannoura & McCorquodale (1985), Gu & Wang (1991) and by van Gent (1992a). The added mass coefficient K_M will be 0.5 for potential flow around an isolated sphere and for a cylinder it will be 1.0. In a densely packed porous medium the coefficient K_M cannot be determined theoretically; most probably it will tend to zero (Madsen, 1974). Van Gent (1993) proposed the following empirical equation

Table 1

Empirical coefficients and characteristic particle diameters for the Forchheimer coefficients a and b (stationary flow)

author	characteristic particle diameter	dimensionless coefficients	
		K_a	K_b
Kozeny (1927); Carman (1937)	d_{eq} ¹⁾	180	— ³⁾
Ergun (1949, 1952)	d_{n50} ²⁾	150	1.75
Engelund (1953)	d_{eq}	— ³⁾	1.8 – 3.6
Koenders (1985)	d_{n15}	250 – 330	— ³⁾
den Adel (1987)	d_{n15}	75 – 350	— ³⁾
Shih (1990)	d_{n15}	> 1684	1.72 – 3.29
van Gent (1993)	d_{n50}	1000	1.1

¹⁾ the equivalent diameter d_{eq} is the diameter of a sphere with mass m_{50} and specific density ϱ_s of an average actual particle: $d_{eq} = (6 m_{50}/\pi \varrho_s)^{1/3}$

²⁾ the nominal diameter d_{n50} is the diameter of a cube with mass m_{50} and specific density ϱ_s of an average actual particle: $d_{n50} = (m_{50}/\varrho_s)^{1/3}$

³⁾ authors proposed a different approach from equations 2 and 3

for the added mass coefficient of a rubble mound. His approach may lead for small velocity amplitudes \tilde{v}_f and long periods T to negative values of K_M , which are physically meaningless and have to be excluded:

$$K_M = \max. \left\{ 0.85 - 0.015 \frac{n g T}{\tilde{v}_f} ; 0 \right\}$$

The hydraulic resistance of a rigid homogeneous, isotropic porous medium can be determined for single phase flow by equation 1 and equations 2, 3 and 4. Using the Forchheimer coefficients an averaged Navier Stokes equation (van Gent, 1992a) reads:

$$c \frac{\partial \vec{v}_f}{\partial t} + \frac{1}{n^2 g} \vec{v}_f \cdot \text{grad } \vec{v}_f = -\text{grad} \left(\frac{p}{\varrho g} + z \right) - a \vec{v}_f - b |\vec{v}_f| \vec{v}_f \quad (5)$$

Neglecting the convective acceleration yields the extended Forchheimer equation (equation 1).

In case of a non-rigid porous medium the combined motion of fluid and particles has to be considered as two-phase flow. For an anisotropic porous medium the Forchheimer coefficients may vary with flow direction. A spatial variation

of Forchheimer coefficients has to be considered for inhomogeneous porous media. The transition between areas with different resistance has to be defined separately. Air entrainment leads to a compressible two-phase flow. A modified Forchheimer equation for two-phase flow (air water mixture) in a porous medium has been proposed by (Hannoura & McCorquodale, 1985).

1.2 Previous work: Pore pressure oscillations in rubble mound breakwaters

The wave propagation in a rubble mound breakwater has been investigated by Hall (1991, 1994) in small scale experiments and by Buerger et al. (1988), Oumeraci & Partenscky (1990) and Muttray et al. (1992, 1995) in large scale experiments. Field measurements have been conducted at the breakwater at Zeebrugge (Troch et al., 1996, 1998), prototype data, experimental data and numerical results have been analysed by Troch et al. (2002).

The water surface elevations inside the breakwater and the amplitude of the pore pressure oscillations decrease in direction of wave propagation exponentially (Hall, 1991; Muttray et al., 1995). However, for larger waves Hall (1991) stated constant maximum water surface elevations in the seaward part of the breakwater core, which might be induced by 'internal wave overtopping' (the wave run-up on the breakwater core reaches the top of the core and causes a downward infiltration from the crest). The water surface elevations, the pore pressure oscillations and the wave set-up increase with increasing wave height, wave period and slope $\cot \alpha$ (Oumeraci & Partenscky, 1990; Hall, 1991). They decrease with increasing permeability of the core material and with increasing thickness of the filter layer (Hall, 1991).

The damping rate of pore pressure oscillations increases with wave steepness (Buerger et al., 1988; Troch et al., 1996) and decreases with increasing distance from the still water line (Oumeraci & Partenscky, 1990; Troch et al., 1996). The following approach has been proposed by Oumeraci & Partenscky (1990) and applied by Burcharth et al. (1999) and Troch et al. (2002) for the damping of pore pressure oscillations:

$$P(x) = P_0 \exp\left(-K_d \frac{2\pi}{L'} x\right) \quad (6)$$

with dimensionless damping coefficient K_d , amplitude of pore pressure oscillations P_0 (at position $x = 0$) and $P(x)$ (at varying position $x > 0$) and wave length L' inside the structure. The exponential decrease has been confirmed in field measurements (Troch et al., 1996).

Numerical models have been developed to study the pore pressure attenuation inside rubble mound breakwaters. Van Gent (1992b) proposed a one-

dimensional model where the hydraulic resistance of the porous medium has been considered by Forchheimer type resistance terms. This model provides a realistic figure of the internal wave damping for a wide range of wave conditions and structures. Troch (2001) developed a numerical wave flume in order to study the pore pressure attenuation inside a rubble mound breakwater (2-dimensional analysis). An incompressible fluid with uniform density has been modelled; the VOF method has been applied to treat the free surface. The Navier Stokes equation has been extended by Forchheimer type resistance terms for the porous flow model. However, the effect of air entrainments into the breakwater core has not been considered. From comparison of numerical results, prototype measurements and experimental results it has been concluded that the wave damping inside a breakwater can be approximated by an exponential function (Troch, 2001; Troch et al., 2002).

1.3 Methodology

This study is based on a theoretical analysis of the wave damping inside a rubble mound breakwater. A simple universal concept for the wave height decay inside the structure is presented.

Large scale experiments have been performed with a rubble mound breakwater of typical cross section in order to validate the theoretical results. A large model scale has been selected to prevent scale effects especially with respect to air entrainment. The hydraulic model tests were intended to provide insight into the physical processes of the wave structure interaction, to confirm the theoretical damping approach and to quantify non-linear effects that had been neglected in the theoretical approach. The final objective is a simple and relatively accurate description of wave damping inside a rubble mound breakwater, which clearly reflects the governing physical processes.

It should be noted that the oscillations of water surface (wave height) and pore pressure ('pore pressure height') are closely linked. The wave kinematics in porous media vary significantly in direction of wave propagation. However, the local wave kinematics (at a specific location) are similar inside and outside the porous medium. A linear relation between the wave height at a specific location and the corresponding height of the pore pressure oscillations at a certain level below SWL has been derived theoretically by Biesel (1950). Thus, a proper description of the wave damping inside a breakwater should be applicable for wave heights and pore pressure oscillations.

The analysis of the wave propagation inside the breakwater core has been restricted to the breakwater part, where the water surface remains inside the core during the entire wave cycle. Thus, only the breakwater core landward

of the point of maximum wave run-up between the filter layer and the core has been considered (figure 1). Further seaward the wave motion inside the breakwater core will be affected by the various layers of the breakwater (with varying permeability) and by the wave motion on the breakwater slope (wave run-up and run-down).

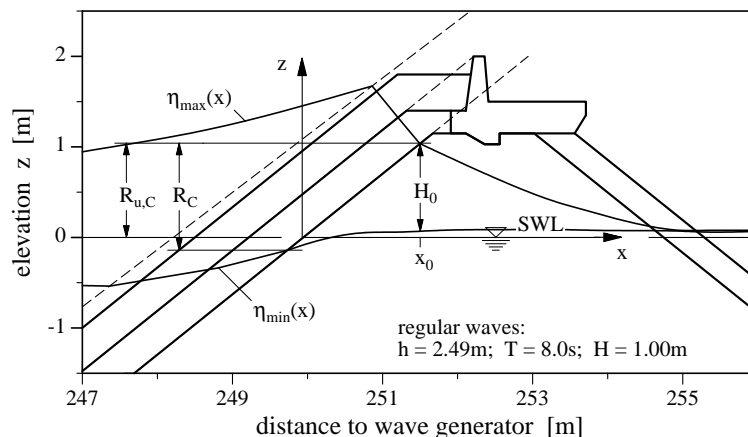


Fig. 1. Definition sketch for the analysis of wave damping inside the breakwater core

The wave height at the point of maximum wave run-up between the core and the filter layer ($x_0 = x(R_{u,max})$) has been considered as the initial wave height H_0 . This procedure is different from previous studies, where the interface between filter layer and core has been considered as x_0 (see for example Buerger et al., 1988; Troch et al., 1996; Burcharth et al., 1999). With the proposed definition of the position x_0 , the wave damping will not be affected by the breakwater geometry but only by the hydraulic resistance of the core material. The wave transformation in the seaward part of the breakwater and the relation between incident wave height, wave run-up and initial wave height H_0 are not subject of this paper. A homogeneous core material has been assumed for the wave damping analysis. It has been further assumed that the wave damping inside the core at $x \geq x_0$ is not directly affected by the wave transformation at the seaward slope (except for the initial wave height H_0). Thus, wave damping inside the breakwater core and the infiltration process at the slope have been considered as two separate and successive processes. The following terminology is used in this paper: Water surface oscillation and pressure oscillation stand for the variation of water surface line and dynamic pressure in time (at a specific location x). Wave height H refers to the vertical distance between wave crest and trough at a specific location x for regular waves and to the significant wave height H_{m0} for irregular waves. Pressure height P corresponds to wave height (derived from pressure oscillations instead of water surface elevations). Wave damping denotes the attenuation of wave height and pore pressure height in direction of wave propagation (x -direction). Deviations between observation and theoretical prediction of a parameter y are quantified

by standard deviation σ_y , relative standard deviation σ_y/\bar{y} (with mean value \bar{y}) and by systematic deviation μ_y (average deviation between observation and prediction).

2 Theoretical approach for wave damping

The relationship between hydraulic gradient I and discharge velocity v_f is determined by the extended Forchheimer equation (equation 1). The wave damping inside a rubble mound breakwater is closely linked to the hydraulic resistance. Various relatively simple approaches for the wave damping inside a rubble mound breakwater have been derived from equation 1.

The discharge velocity $v_f(x, z, t)$ has been replaced by a depth averaged ($z = 0 \rightarrow -h$) and time averaged ($t = 0 \rightarrow T$) velocity $\bar{v}_f(x)$. The averaged particle velocities inside the breakwater $\bar{v}_f(x)$ can be approximated according to Muttray (2000) by:

$$\bar{v}_f(x) = \kappa_v H(x) \quad (7)$$

$$\kappa_v = \frac{n}{\pi} \frac{\omega}{k'h} \left[1 + \frac{2}{\pi} \left(1 - \frac{\cosh k'h}{\cosh 1.5 k'h} \right) \right] \quad (8)$$

with local wave height $H(x)$, circular frequency $\omega = 2\pi/T$, internal wave number $k' = 2\pi/L'$ (internal wave length L'), water depth h and porosity n . The velocity coefficient $\kappa_v [s^{-1}]$ has been introduced for convenience only.

The hydraulic gradient $\bar{I}(x)$ (averaged over water depth and wave period) corresponds to the averaged pressure gradient if the water depth is constant. The gradient $\bar{I}(x)$ will be equal to the gradient of the pressure height $\partial\bar{P}(x)/\partial x$ and to the gradient of the wave height $\partial H(x)/\partial x$ if the oscillations of water surface and pore pressure (variation in time at a fixed location) are sinusoidal and if possible variations of pore pressure oscillations over the water depth are neglected:

$$\bar{I}(x) = -\text{grad} \left(\frac{\bar{p}(x)}{\rho g} \right) = -\frac{2}{\pi} \frac{\partial \bar{P}(x)}{\partial x} = -\frac{2}{\pi} \frac{\partial H(x)}{\partial x} \quad (9)$$

With hydraulic resistance $\bar{I}(x)$ according to equation 9 and discharge velocity \bar{v}_f according to equation 7 the Forchheimer equation (with $\partial(\kappa_v H)/\partial t = 0$) reads:

$$-\frac{2}{\pi} \frac{\partial H(x)}{\partial x} = a \kappa_v H(x) + b (\kappa_v H(x))^2 \quad (10)$$

The resulting damping function will be linear, quadratic or polynomial and depends on the actual flow properties.

Linear damping: For laminar flow, the relation between hydraulic gradient and discharge velocity is linear (Darcy's law). A linear dependency between wave height decay and wave height is called linear damping. If non-linear hydraulic resistance is neglected equation 10 reduces to:

$$-\frac{2}{\pi} \frac{\partial H(x)}{\partial x} = a \kappa_v H(x)$$

Separation of variables and integration leads to:

$$H(x) = \exp\left(-\frac{\pi}{2} a \kappa_v x + C\right)$$

A linear damping thus results in an exponential decrease of wave height. The integration constant C can be determined from the boundary conditions if the initial wave height is $H(x = 0) = H_0$:

$$C = \ln(H_0)$$

and the wave height decay due to linear damping is finally described by:

$$H(x) = H_0 \exp\left(-\frac{\pi}{2} a \kappa_v x\right) \quad (11)$$

Quadratic damping: The hydraulic gradient in fully turbulent flow is in proportion to the discharge velocity squared. A wave height decay that depends on the wave height squared is called quadratic damping. If the linear hydraulic resistance is neglected equation 10 leads to the following quadratic damping function:

$$\begin{aligned} -\frac{2}{\pi} \frac{\partial H(x)}{\partial x} &= b (\kappa_v H(x))^2 \\ H(x) &= \frac{1}{\frac{\pi}{2} b \kappa_v^2 x - C} \quad \text{with: } C = -\frac{1}{H_0} \\ H(x) &= \frac{H_0}{\frac{\pi}{2} b \kappa_v^2 H_0 x + 1} \end{aligned} \quad (12)$$

Polynomial damping: The hydraulic gradient can be described by the Forchheimer equation if turbulent and laminar flow both occur in the porous medium. A wave height decay that depends on the wave height and on the wave height squared is called polynomial damping. Equation 10 leads to the following polynomial damping function:

$$\begin{aligned}
 -\frac{2}{\pi} \frac{\partial H(x)}{\partial x} &= a \kappa_v H(x) + b (\kappa_v H(x))^2 \\
 H(x) &= \frac{\pi a \kappa_v}{2 \exp \left[\frac{\pi}{2} a \kappa_v (x + C) \right] - \pi b \kappa_v^2} \\
 \text{with: } C &= \frac{2}{\pi a \kappa_v} \ln \left[\frac{\pi}{2} \kappa_v \left(\frac{a}{H_0} + b \kappa_v \right) \right] \\
 H(x) &= \frac{a}{\left(\frac{a}{H_0} + b \kappa_v \right) \exp \left(\frac{\pi}{2} a \kappa_v x \right) - b \kappa_v} \quad (13)
 \end{aligned}$$

The various damping functions are plotted in figure 2; the coefficients a and b and the initial wave heights H_0 that have been used are listed in table 2.

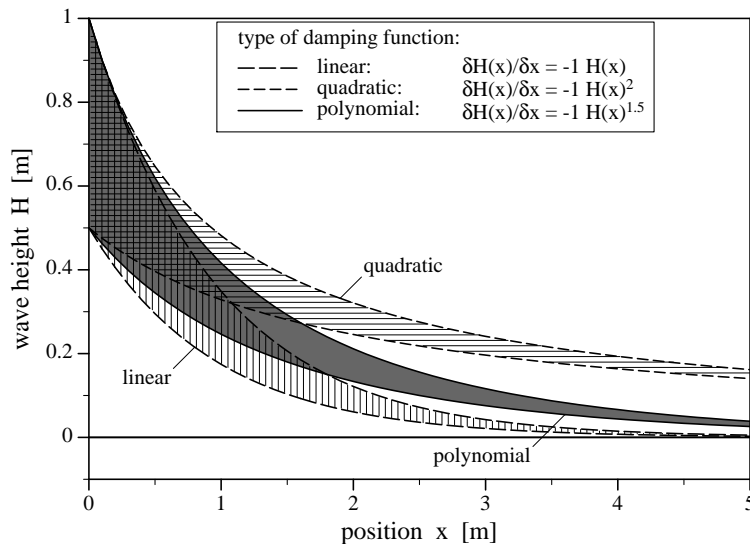


Fig. 2. Linear, quadratic and polynomial damping

Two waves with initial wave heights H_0 (at position $x = 0$) of 1 m and 0.5 m are considered (see figure 2). The ratio of the local wave heights $H(x)$ (at position $x > 0$) will be constant ($= 0.5$) for linear damping. Quadratic damping will cause a stronger wave height reduction for the larger wave and consequently, the ratio of the local wave heights will vary (from 0.5 to 1). A similar effect can be seen for polynomial damping, which of course depends on the relative importance of the quadratic resistance.

Table 2
Hydraulic resistance coefficients and initial wave heights¹⁾

damping- function	coefficient a [s/m]	coefficient b [s ² /m ²]	initial wave height H_0 [m]
linear	$2/(\pi \kappa_v)$	–	0.5 – 1.0
quadratic	–	$2/(\pi \kappa_v^2)$	0.5 – 1.0
polynomial	$1/(\pi \kappa_v)$	$1/(\pi \kappa_v^2)$	0.5 – 1.0

¹⁾ applied in figure 2

Table 3
Geometric properties of core material (van Gent, 1993)

equivalent diameter	$d_{eq} = 0.0385 m$	$d_{eq} = (6 m_{50}/\pi \rho_s)^{1/3}$
nominal diameter	$d_{n15} = 0.023 m$	$d_{ni} = (m_i/\rho_s)^{1/3}$
	$d_{n50} = 0.031 m$	
	$d_{n85} = 0.040 m$	
non-uniformity	$d_{n60}/d_{n10} = 1.51$	
porosity	$n = 0.388$	

3 Experimental investigations

3.1 Experimental set-up and test procedure

The experimental set-up in the Large Wave Flume (GWK) in Hanover consisted of a foreshore (length 100 m, 1:50 slope) and a rubble mound breakwater of typical cross section with Accropode armour layer, underlayer, core, toe protection and crest wall. The breakwater had 1:1.5 slopes and the crest level was at 4.50 m above seabed (figure 3).

The breakwater core had a crest width of 1.35 m and a crest height of 3.75 m (figure 3). The core material consisted of gravel (rock size 22/56 mm); the geometric properties of the core material are summarised in table 3.

The resistance coefficients of the extended Forchheimer equation for oscillating single phase flow inside the breakwater core are summarised in table 4 as well as the their contribution to the total flow resistance. The coefficients for the core material have been determined experimentally for stationary and oscillatory flow conditions that were similar to the tested flow conditions inside the breakwater.

Table 4

Resistance coefficients for the core material and contribution to the total flow resistance for oscillatory flow

laminar resistance coeff. a [s/m]	resistance contri- bution [%]	turbulent resistance coeff. b [s^2/m^2]	resistance contri- bution [%]	inertia force coeff. c [s^2/m]	force contri- bution [%]
0.89	11	22.9	83 – 87	0.26	2 – 6

The wave motion on the breakwater slope, which is governing the hydraulic processes inside the structure, was measured including wave run-up, pressure distribution on the slope and water surface elevations. The wave propagation inside the structure has been determined from the water surface elevations inside the core (wave gauges 22–26) and at the boundaries between different layers (wave run-up gauges 2 & 3). The pore pressure distribution was measured inside the core (at three different levels: pressure cells 1–7, 8–13, 14–18) and along the boundaries of the various layers (pressure cells 24–28 and 19–23). The positions of the measuring devices at and inside the rubble mound breakwater are specified in figure 3.

For wave height measurements inside the structure the wave gauges were protected by a cage against the surrounding rock material. Pressure sensors of type Druck PDCR 830 were used. For pore pressure measurements, the pressure cells were protected by a plastic shell.

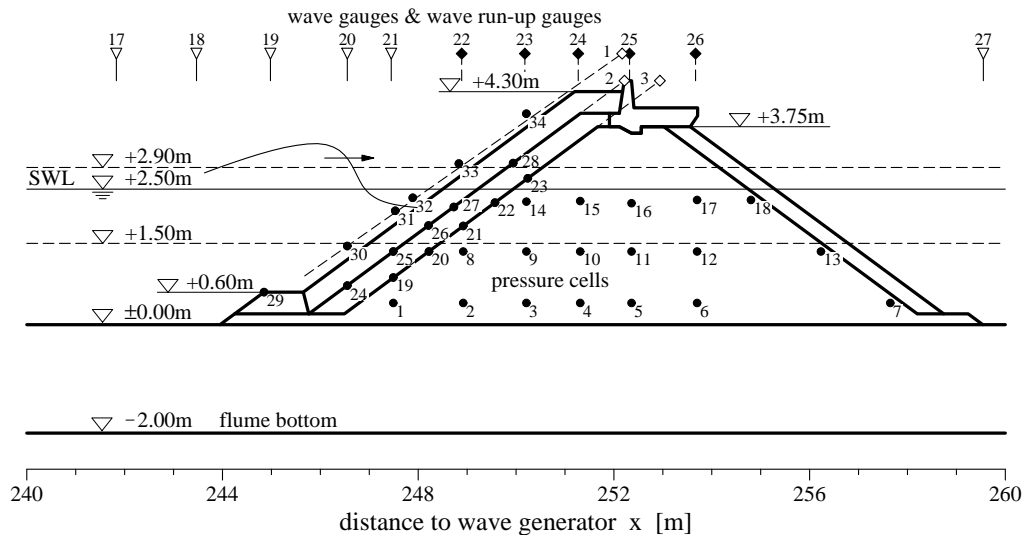


Fig. 3. Cross section of the breakwater model with measuring devices: wave gauges, wave run-up gauges and pressure cells

A typical breakwater configuration has been selected for the model tests in the GWK; the structural parameters (geometry and rock material) have not

Table 5
Wave conditions tested

water level h [m]	wave period T, T_p [s]	regular waves		wave spectra	
		incident wave height ¹⁾ H_i [m]	initial wave height ²⁾ H_0 [m]	incident wave height ¹⁾ $H_{i,m0}$ [m]	initial wave height ²⁾ $H_{0,m0}$ [m]
2.50	4	0.23 – 0.81	0.15 – 0.78	0.24 – 0.78	0.15 – 0.34
2.50	5	0.26 – 1.06	0.19 – 0.98	0.25 – 0.98	0.19 – 0.49
2.50	6	0.27 – 1.09	0.23 – 1.04	0.25 – 1.04	0.21 – 0.60
2.50	8	0.28 – 1.25	0.28 – 1.06	0.26 – 1.06	0.27 – 0.77
2.50	10	0.60	0.59		
2.90	3	0.22 – 0.60	0.11 – 0.21	0.22 – 0.47	0.11 – 0.18
2.90	4	0.23 – 0.70	0.14 – 0.31	0.23 – 0.64	0.14 – 0.29
2.90	5	0.25 – 0.70	0.18 – 0.38	0.24 – 0.68	0.18 – 0.37
2.90	6	0.26 – 0.73	0.22 – 0.46	0.26 – 0.71	0.22 – 0.45
2.90	8	0.27 – 0.78	0.27 – 0.61	0.26 – 0.73	0.26 – 0.58
2.90	10	0.27 – 0.81	0.31 – 0.73	0.27 – 0.58	0.31 – 0.57

¹⁾ at the toe of the breakwater

²⁾ inside the breakwater core

been varied with respect to the large model scale. The wave parameters have been varied systematically (see table 5).

Two water levels ($h = 2.50\text{ m}$ and 2.90 m) have been tested. At the lower water level ($h = 2.50\text{ m}$) most of pressure cells were permanently submerged, thus providing a complete picture of the pore pressure oscillations. Wave overtopping was practically excluded from these tests in order to avoid any infiltration into the breakwater core from the breakwater crest. Therefore the wave heights at water level $h = 2.50\text{ m}$ and 2.90 m were limited to $H = 1.00\text{ m}$ and 0.70 m , respectively.

Tests were conducted with both regular and irregular waves. The regular wave tests were used to provide insight into the hydraulic processes, but also to validate the theoretical approaches and to develop empirical adjustments and extensions. Tests with irregular waves (TMA-wave spectra generated from JONSWAP-spectra) were used to check the applicability of regular wave results for irregular waves and if necessary to adapt it.

The wave conditions that have been tested are summarised in table 5. The relative water depth h/L varied from 0.05 to 0.23 ($kh = 0.35$ to 1.45) and

was thus transitional and close to shallow water conditions. The wave steepness ($H/L = 0.005$ to 0.056) was significantly lower than the limiting wave steepness for progressive waves ($(H/L)_{crit} \approx 0.14$) and also the relative wave height ($H/h = 0.09$ to 0.4) was significantly lower than the critical wave height ($(H/h)_{crit} \approx 0.8$). The surf similarity parameter $\xi = \tan \alpha / \sqrt{H/L_0}$ varied from 3.0 to 16.7 . The ratio of initial and incident wave height H_0/H_i was 0.35 to 1.14 (on average 0.68). Typical results of the hydraulic model tests are plotted in figure 4 showing the water surface line and the pressure distribution inside the breakwater just before maximum wave run-up.

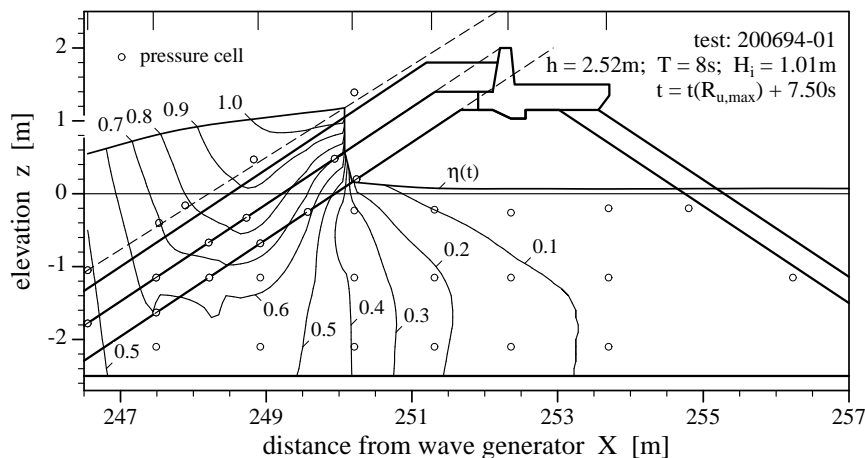


Fig. 4. Lines of constant pressure heights $p/\rho g$ [m] inside the breakwater during wave run-up (regular wave, $T = 8$ s, $H_i = 1.01$ m, $h = 2.52$ m)

3.2 Experimental results

The wave height inside the breakwater core is plotted in figure 5 against the distance $x - x_0$ (see figure 1) for regular waves (wave periods $T = 4$ s, 8 s, nominal incident wave heights (in front of the breakwater) $H = 0.25$ m, 0.40 m, 0.55 m, 0.70 m and water level $h = 2.50$ m). The initial wave height H_0 at position x_0 varies with incident wave height and with wave period. For shorter waves ($T = 4$ s) the wave height inside the breakwater core $H(x)$ approaches after a relatively short distance a value that is almost independent of the initial wave height H_0 . Once this value is reached the wave damping is significantly reduced. A similar effect (decreasing variation of local wave heights and decreasing wave damping) can also be seen for longer waves ($T = 8$ s).

The varying ratio of the local wave heights (see figures 2 and 5) gives some indication that the wave damping inside a breakwater will be better approximated by a quadratic or polynomial damping function than by the linear damping function. The applicability of the damping functions (equations 11,

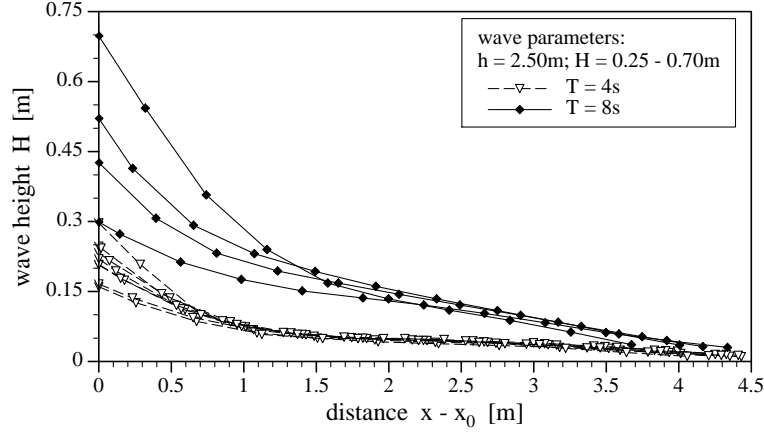


Fig. 5. Variation of wave height inside the core with distance $x - x_0$ for various incident wave heights and wave periods

12 and 13) for the wave height attenuation inside a breakwater is addressed below. The velocity coefficient κ_v according to equation 8 was almost constant ($\kappa_v \approx 0.25 \text{ s}^{-1}$ with a standard deviation $\sigma_{\kappa_v} = 0.011 \text{ s}^{-1}$ (4.5 %)) for the wave conditions that have been tested (see table 5).

Linear damping: The linear damping approach (equation 11) uses a resistance coefficient a , which corresponds to the Forchheimer coefficient a for laminar flow. However, for turbulent flow the linear Forchheimer coefficient will not be applicable. As the flow pattern inside a breakwater is governed by turbulent flow the coefficient a has been replaced by a coefficient a_{eq} that takes laminar and turbulent resistance into account. The coefficient a_{eq} has been derived by a linearisation, i.e. integration and averaging of the actual flow resistance. A rational approximation for the linearised resistance coefficient has been proposed by Muttray (2000):

$$a_{eq} = a + \frac{1}{36} \bar{H} \frac{gb}{\sqrt{ch}} \left[1 + \frac{k'h}{4} - \frac{2}{5} \tanh k'h \right] \quad (14)$$

with average wave height \bar{H} inside the breakwater core and internal wave number k' , which has been assessed from a linearised dispersion equation for wave motion in porous media:

$$\omega^2 = \frac{k'}{nc} \tanh(k'h) \quad (15)$$

The coefficient a_{eq} has been determined iteratively. A starting value for a_{eq} has been derived from equation 14 with $\bar{H} = H_0$ (see table 5) and coefficients

a , b and c according to table 4. The wave height inside the breakwater $H(x)$ has been determined subsequently from equation 11. The average wave height \bar{H} (averaged over the width of the breakwater) has finally been used to re-calculate a_{eq} from equation 14.

The width of the breakwater core that has been tested varied at SWL between 3.9 m and 5.1 m (depending on the water level); a distance of 3 m has been considered for the assessment of the average wave height \bar{H} . For the wave conditions tested the average internal wave height was about $\bar{H} = 0.43 H_0$. The resistance coefficient a_{eq} varied between 1.2 and 3.6 and was on average 2 with standard deviation $\sigma_a = 0.55 \text{ s/m}$ (27%).

The applicability of the linear damping approach (equation 11) for the decrease of wave height inside the breakwater core is demonstrated in figure 6.

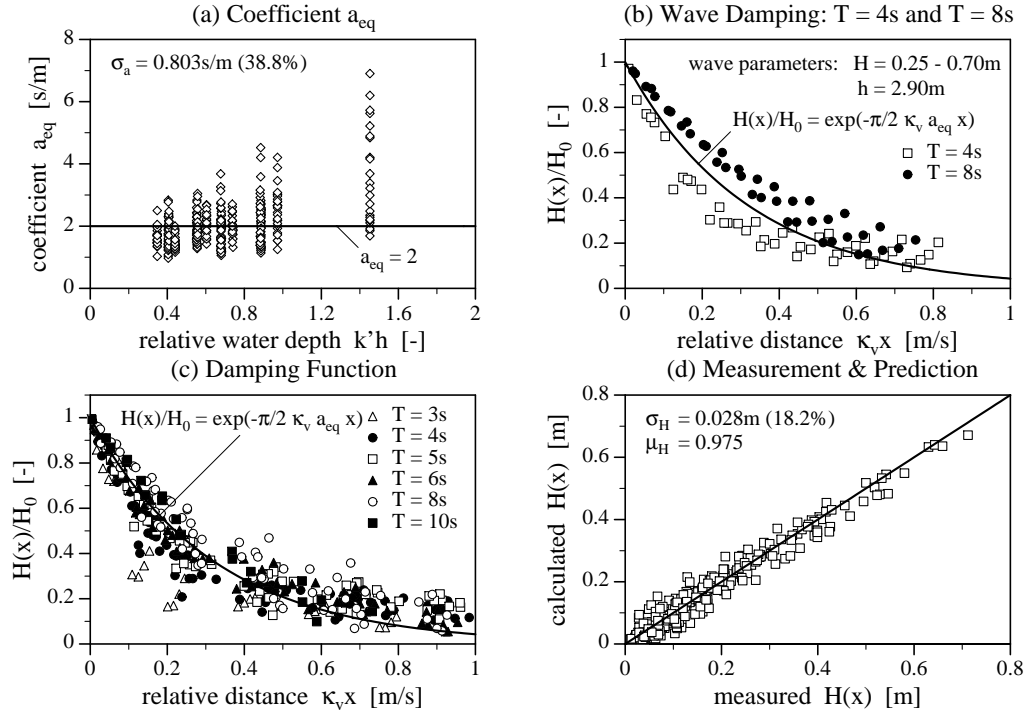


Fig. 6. Linear wave damping approach: (a) damping coefficient a derived from measurements, (b) wave decay for longer ($T = 8 \text{ s}$) and shorter ($T = 4 \text{ s}$) wave periods, (c) wave decay vs. relative distance $\kappa_v x$ and (d) comparison of measured and calculated local wave heights $H(x)$

In figure 6 a the coefficient a_{eq} that has been derived from equation 11 (with measured wave heights H_0 and $H(x)$) is plotted against the relative water depth $k'h$. The coefficient a_{eq} is on average 2 s/m ; the standard deviation σ_a is 0.803 s/m (38.8%). The theoretical assessment of the linearised resistance coefficient a_{eq} (iterative procedure) is confirmed by these results.

The differences between measured and calculated wave height decay (accord-

ing to equation 11) are shown for a number of tests with shorter and longer wave periods ($T = 4\text{ s}$ and $T = 8\text{ s}$, $H_i = 0.25 - 0.70\text{ m}$ and $h = 2.90\text{ m}$) in figure 6 b (with $a_{eq} = 2\text{ s/m}$ and $\kappa_v \approx 0.25\text{ s}^{-1}$). The wave height attenuation of longer waves ($T = 8\text{ s}$) is overestimated in the seaward part of the breakwater core ($\kappa_v x \leq 0.3$) while the wave damping of shorter waves ($T = 4\text{ s}$) is underestimated.

The wave height evolution inside the core is plotted in figure 6 c against the relative distance $\kappa_v x$ for all tests. The non-dimensional distance $\kappa_v x$ is a governing parameter for the wave attenuation according to the linear damping approach (equation 11). It can be seen that the wave heights in the landward part of the breakwater core ($\kappa_v x \geq 0.6$) are underestimated.

A direct comparison of measured and calculated wave heights inside the structure is plotted in figure 6 d for all tests. The measured wave heights are on average 2.5 % smaller than the calculated wave heights; the standard deviation is $\sigma_H = 0.028\text{ m}$ (18.2 %).

Even though the actual wave height decay inside the structure shows some systematic differences as compared to the calculated decay according to equation 11, the linear damping approach provides a very simple and relatively accurate approximation for the wave damping inside the breakwater core (see figures 6 c,d).

Quadratic damping: The applicability of the quadratic damping approach according to equation 12 for the wave height decay inside the breakwater core is shown in figure 7.

The quadratic damping coefficient b that has been derived from equation 12 (with measured wave heights H_0 and $H(x)$) is plotted in figure 7 a against the relative water depth $k'h$. The coefficient b is increasing with $k'h$ and has been approximated empirically by equation 3 and $\kappa_o K_b = 3.4 k'h$. The standard deviation between observed and calculated coefficients b is $\sigma_b = 42.4\text{ s}^2/\text{m}^2$ (86.1 %). The Forchheimer coefficient $b = 22.9\text{ s}^2/\text{m}^2$ that has been determined experimentally (see table 4) is plotted for comparison.

The differences between measured and calculated wave height decay (according to equation 12) are shown for a number of tests with shorter and longer wave periods in figure 7 b (see also figure 6 b). The decrease of wave height is plotted against $\kappa_v^2 H_0 x$. The damping coefficient b varies with $k'h$; the wave damping is therefore different for longer and shorter waves.

The wave damping inside the breakwater is plotted in figure 7 c against the relative distance $b\kappa_v^2 H_0 x$ for all tests. The non-dimensional distance $b\kappa_v^2 H_0 x$ is a governing parameter of the quadratic damping approach (equation 12). The

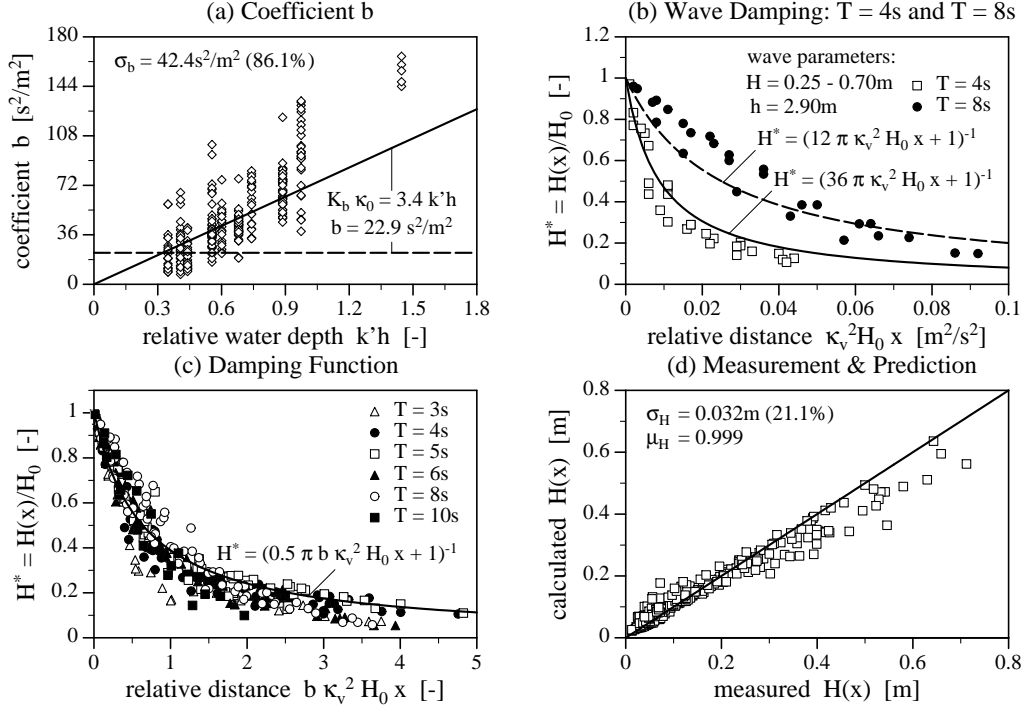


Fig. 7. Quadratic wave damping approach: (a) damping coefficient b derived from measurements, (b) wave decay for longer ($T = 8 \text{ s}$) and shorter ($T = 4 \text{ s}$) wave periods, (c) wave decay vs. relative distance $b \kappa_v^2 H_0 x$ and (d) comparison of measured and calculated local wave heights $H(x)$

wave heights in the seaward part of the structure ($b \kappa_v^2 H_0 x \leq 0.5$) are slightly underestimated while the wave heights in the landward part ($b \kappa_v^2 H_0 x > 1$) are slightly overestimated.

A direct comparison of measured and predicted wave heights (equation 12) can be seen in figure 7d for all tests. The systematic deviation between measured and calculated values is only 0.1%, the standard deviation is $\sigma_H = 0.032 \text{ m}$ (21.1%). Major differences can be seen for larger wave heights ($H(x) > 0.3 \text{ m}$), therefore the goodness of fit is slightly less than for the linear damping approach.

If the Forchheimer coefficient $b = 22.9 \text{ s}^2/\text{m}^2$ (see table 4) is applied as a damping coefficient in equation 12 the wave height inside the structure will be overestimated on average by 16.3%. The standard deviation between measured and predicted wave heights will be increased to $\sigma_H = 0.052 \text{ m}$ (33.9%).

The wave decay inside the breakwater is qualitatively better reproduced by the quadratic damping function than by the linear damping model (see figures 6b and 7b). However, the effect of wave length is apparently not properly described by the velocity coefficient κ_v . This shortcoming will affect the results from the quadratic approach more than the results of the linear approach (κ_v is linear in equation 11 and quadratic in equation 12). Even though the

quadratic approach covers more of the physics of the wave damping process inside a breakwater than the linear approach it does not provide a better prediction of the wave height attenuation.

The shortcomings of the velocity coefficient κ_v can be partly compensated by an empirical correction of coefficient b (with $\kappa_o K_b = 3.4k'h$). For the present case the relative standard deviation has been reduced from 33.9% to 21.1%. However, the general applicability of such purely empirical procedure is uncertain.

In the landward part of the breakwater the wave heights are underestimated by the linear damping approach and overestimated by the quadratic approach. Thus, a polynomial approach according to equation 13 that contains a linear and quadratic contribution might be a better alternative.

Polynomial damping: The applicability of the polynomial damping approach according to equation 13 is shown in figure 8.

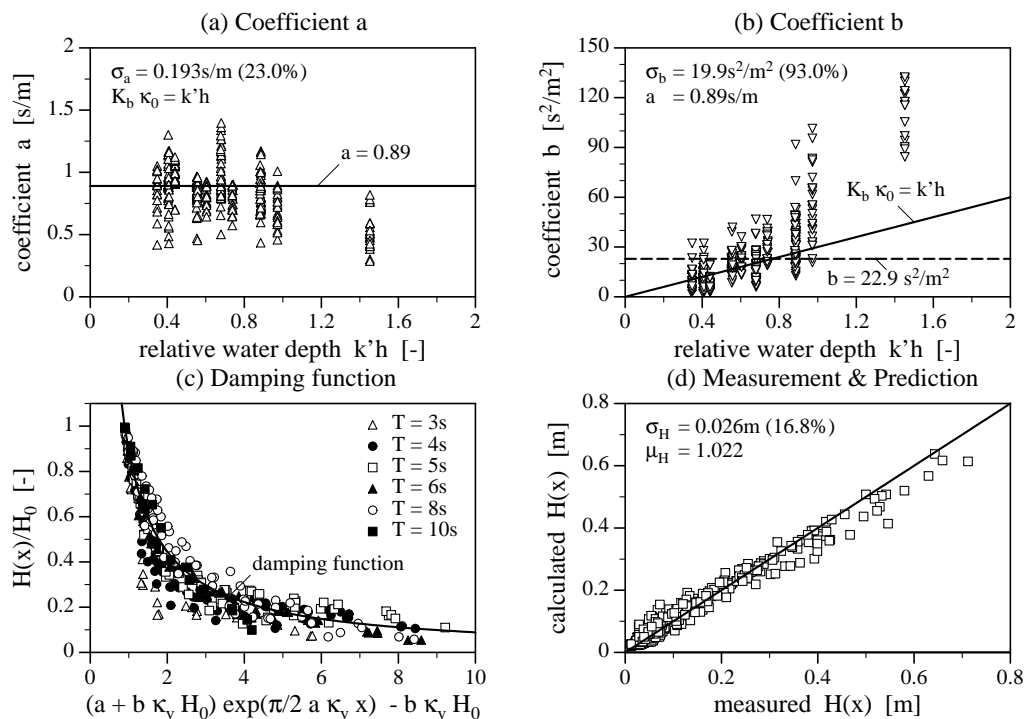


Fig. 8. Polynomial wave damping approach: (a) linear damping coefficient a derived from measurements, (b) quadratic damping coefficient b derived from measurements, (c) wave decay inside the breakwater core and (d) comparison of measured and calculated local wave heights $H(x)$

The linear and quadratic resistance coefficients a and b are plotted in figure 8 a and figure 8 b against the relative water depth $k'h$. The Forchheimer coefficient $a = 0.89 \text{ s/m}$ (see table 4) has been applied as linear damping coefficient.

The standard deviation between coefficients a that have been deduced from measurements (with empirically corrected coefficient b) and the nominal value $a = 0.89 \text{ m/s}$ is $\sigma_a = 0.193 \text{ s/m}$ (23.0%). The quadratic damping coefficient b has been corrected empirically in order to compensate the effect of wave length that is not sufficiently taken into account by the coefficient κ_v . Coefficient b is determined by equation 3; as for the quadratic damping approach the coefficients κ_o and K_b have been adjusted ($\kappa_o K_b = k'h$). The standard deviation between the modified coefficient b and the coefficients that have been derived from measurements is $\sigma_b = 19.9 \text{ s}^2/\text{m}^2$ (93.0%, with $a = 0.89 \text{ s/m}$).

The wave decay inside the breakwater core (according to equation 13) is plotted in figure 8c against the relative distance $(a + b \kappa_v H_0) \exp(0.5 \pi a \kappa_v x) - b \kappa_v H_0$. The wave heights in the most seaward part of the structure are slightly underestimated by the polynomial approach while the wave heights in the landward part of the structure are approximated very well.

A direct comparison of measured and predicted wave heights is plotted in figure 8d. The calculated wave heights are on average 2.2% larger than the measured values and have a standard deviation $\sigma_H = 0.026 \text{ m}$ (16.8%). The largest wave heights ($H > 0.4 \text{ m}$) in the most seaward part of the breakwater core are underestimated.

If the experimentally determined linear and quadratic Forchheimer coefficients ($a = 0.89 \text{ s/m}$ and $b = 22.9 \text{ s}^2/\text{m}^2$) are applied the wave heights inside the breakwater will be overestimated on average by 8.0%, the standard deviation is increased to 0.046 m (32.7%).

The polynomial approach according to equation 13 (with an empirical adaptation of the quadratic resistance coefficient b) provides a good approximation of the actual wave height decay inside a breakwater. However, the accuracy of the results is limited by the coefficient κ_v , which does not cover the effect of wave length completely.

Extended polynomial approach: In order to consider the effect of wave length on the wave damping properly an empirical coefficient κ_x is added to the damping approach according to equation 13:

$$H(x) = \frac{a}{\left(\frac{a}{H_0} + b \kappa_v\right) \exp\left(\frac{\pi}{2} a \kappa_v \kappa_x x'\right) - b \kappa_v} \quad (16)$$

with: $x' = x - x_0$

For *regular waves*, the wave decay inside the breakwater core according to

equation 16 is plotted in figure 9. The experimentally derived Forchheimer coefficients $a = 0.89 \text{ s/m}$ and $b = 22.9 \text{ s}^2/\text{m}^2$ (see table 4), an internal wave number k' (equation 15) and the following coefficient κ_x have been applied:

$$\kappa_x = 1.5 k' h \quad (17)$$

The standard deviation between equation 17 and coefficients κ_x that have been derived from measurements is $\sigma_{\kappa_x} = 0.385$ (34.3 %)(figure 9 a). The local wave heights inside the structure according to equation 16 are on average 0.6 % larger than the measured wave heights, the standard deviation is $\sigma_H = 0.021 \text{ m}$ or 14.9 % (figure 9 b). From figure 9 c it can be seen that the actual wave height decay inside a breakwater core is well described by the extended polynomial approach (equation 16).

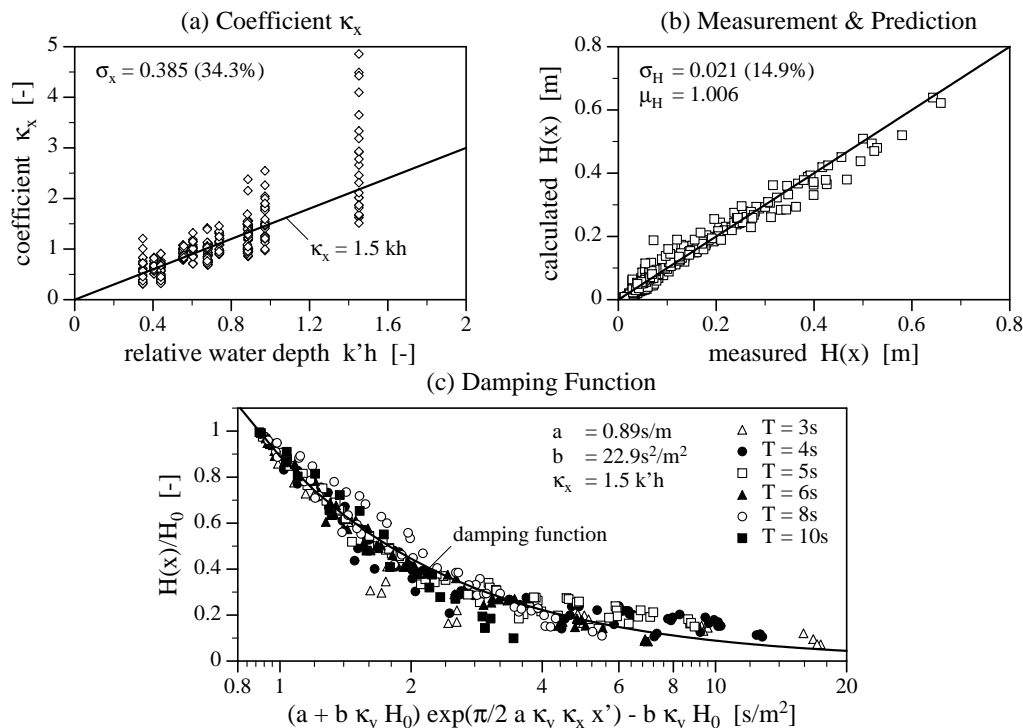


Fig. 9. Extended polynomial wave damping approach for regular waves: (a) coefficient κ_x vs. relative water depth $k'h$, (b) comparison of measured and calculated local wave heights $H(x)$ and (c) wave decay inside the breakwater core

For *wave spectra*, the decay of significant wave heights inside the breakwater is plotted in figure 10. The extended polynomial approach according to equation 16 has been applied. The experimentally derived Forchheimer coefficients $a = 0.89 \text{ s/m}$ and $b = 22.9 \text{ s}^2/\text{m}^2$ and an internal wave number k' have been used as for regular waves. The coefficient κ_x has been slightly modified:

$$\kappa_x = 1.25 k' h \quad (18)$$

The standard deviation between equation 18 and coefficients κ_x that have been derived from measurements is $\sigma_{\kappa_x} = 0.226$ or 25.9% (figure 10 a). The calculated local wave heights inside the structure are on average 2.6% smaller than the measured wave heights, the standard deviation is $\sigma_H = 0.039\text{ m}$ or 29.5% (figure 10 b). The relative wave height inside the structure $H_{m0}(x)/H_{0,m0}$ is plotted in figure 10 c against the relative distance. The wave heights in the seaward part of the breakwater are slightly overestimated while the wave heights in the landward part are slightly underestimated. In some of the experiments with wave periods $T_p = 5\text{ s}$, 6 s and 8 s , the wave height measurements are distorted by "internal wave overtopping" (the wave run-up at the intersection between filter layer and core reaches the crest level of the breakwater core and generates an additional water surface for the wave gauges in this part of the breakwater). Thus it appears as if these waves were propagating a certain distance into the breakwater without significant damping. In all cases without "internal wave overtopping" the decay of significant wave heights H_{m0} inside the breakwater can be reasonably assessed by equation 16 for irregular waves.

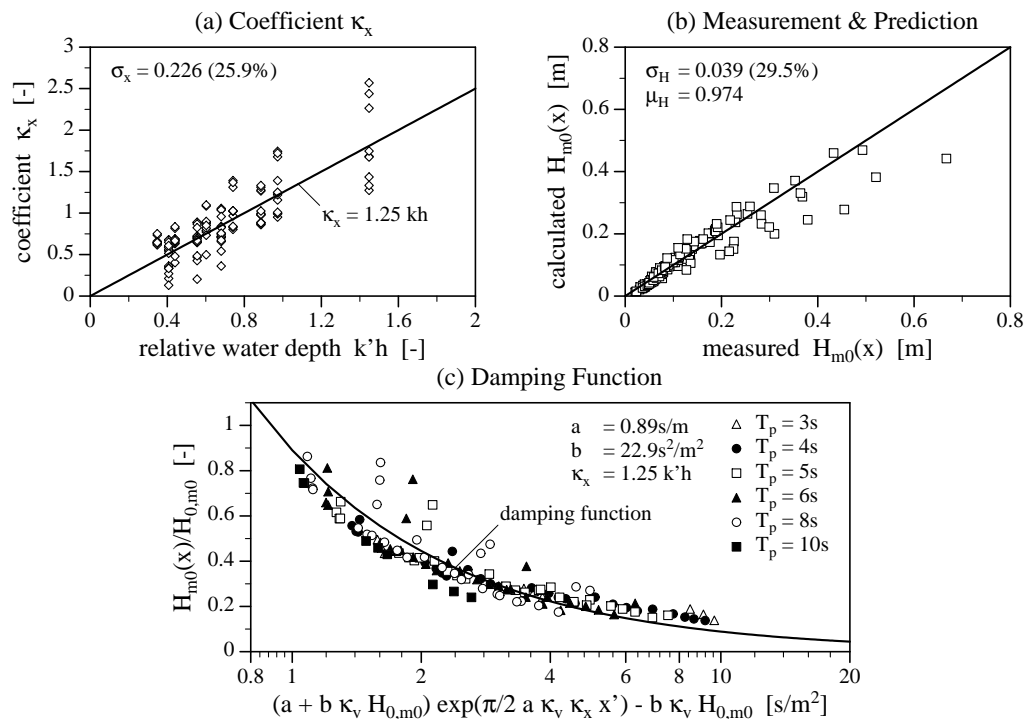


Fig. 10. Extended polynomial wave damping approach for wave spectra: (a) coefficient κ_x vs. relative water depth $k'h$, (b) comparison of measured and calculated local wave heights $H_{m0}(x)$ and (c) wave decay inside the breakwater core

4 Concluding remarks

The wave damping inside a rubble mound breakwater has been studied theoretically and experimentally.

The theoretical concept has been based on the assumption of a homogeneous core material. The wave kinematics have been derived from linear wave theory and the wave length inside the structure has been determined from a linearised dispersion equation for porous media. An average discharge velocity has been considered (averaged over wave period and water depth). The hydraulic gradient has been approximated by the gradient of wave or pressure height. It has been further assumed that the actual hydraulic resistance can be approximated either by a linear, a quadratic or by a polynomial (linear and quadratic) resistance. The effect of non-stationary flow (drag force) has not been considered explicitly. Despite these assumptions and simplifications the damping functions that have been derived from above analysis reflect the governing physical processes better than available approaches such as equation 6.

The actual wave damping can be well described by a linear damping model and the corresponding exponential decrease. The linear Forchheimer coefficient a is not appropriate and has been replaced by an equivalent linear damping coefficient a_{eq} , which takes both laminar and turbulent losses into account and has to be determined iteratively.

A quadratic damping model with a damping coefficient that corresponds to the quadratic Forchheimer coefficient b does not provide any significant improvement while a polynomial approach appears to be very promising. The polynomial approach is mainly advantageous due to the fact that Forchheimer coefficients a and b can be directly applied as damping coefficients in the polynomial model. It was found that the polynomial damping model underestimates the effect of wave length. Thus, an empirical correction has been applied (extended polynomial approach, equation 16) that compensates the shortcomings of the theoretical approach with respect to averaged discharge velocity and linearised dispersion equation.

The extended polynomial damping model (with empirical corrections according to equation 17 and equation 18) is applicable for regular and irregular waves if the hydraulic resistance of the porous medium can be approximated by the Forchheimer equation. Thus, the new approach is not restricted to certain breakwater geometries or wave conditions. However, in the case of wave overtopping or "internal wave overtopping" (infiltration into the core from the breakwater crest) the pressure distribution inside the breakwater and the internal wave decay may differ significantly from the proposed model.

5 Acknowledgements

The support of the German Research Foundation (DFG) within the Basic Research Unit SFB 205, project B13 ("Design of rubble mound breakwaters") and within the research programme "Design wave parameters for coastal structures" (Ou 1/3-1,2,3) is gratefully acknowledged. Further the essential contributions of Christian Pabst amongst many others in the experimental study, of Erik Winkel in the data analysis and of Dr. Deborah Wood in the theoretical study shall be mentioned.

References

- Adel, H. den (1987): Re-analysis of permeability measurements using Forchheimer's equation. Delft Geotechnics, Report C0-272550/56.
- Biesel, F. (1950): Equations de l'écoulement non lent en milieu perméable. *Houille Blanche*; No. 2, pp. 157.
- Bruun, P.; Johannesson, P. (1976): Parameters affecting stability of rubble mounds. ASCE; *Journal of Waterways, Harbors and Coastal Engineering Division*; Vol. 102, No. 2, pp. 141–165;
- Burcharth, H.F.; Andersen, O.H. (1995): On the one-dimensional steady and unsteady porous flow equations. *Coastal Engineering*; Vol. 24, pp. 233–257; Elsevier Science Publishers B.V., Amsterdam.
- Burcharth, H.F.; Liu, Z.; Troch P. (1999): Scaling of core material in rubble mound breakwater model tests. *Proceedings Coastal and Port Engineering in Developing Countries (COPEDEC)*; Vol. 5, pp. 1518–1528; Cape Town, South Africa.
- Buerger, W.; Oumeraci, H.; Partenscky, H.W. (1988): Geohydraulic investigations of rubble mound breakwaters. ASCE; *Proceedings International Conference Coastal Engineering (ICCE)*; Vol. 21, pp. 15; Malaga, Spain.
- Carman, P.C. (1937): Fluid flow through granular beds. *Trans. Inst. of Chemical Eng.*; Vol. 15, pp. 150–166; London.
- Engelund, F.A. (1953): On the laminar and turbulent flow of groundwater through homogeneous sand. *Transactions Danish Academy of Technical Sciences*; Vol. 3, No. 4, pp. 1.
- Ergun, S.; Orning, A.A. (1949): Fluid flow through randomly packed columns and fluidized beds. *Journal of Industrial Eng. Chemistry*; Vol. 41, No. 6, pp. 1179–1189.
- Ergun, S. (1952): Fluid flow through packed columns. *Chem. Engrg. Progress*; Vol. 48, pp. 89–94.
- Gent, M.R.A. van (1992): Formulae to describe porous flow. Faculty of Civil Engineering; *Communications on Hydraulic and Geotechnical Engineering*; Report No. 92–2; pp. 50; Delft University of Technology, Delft.

- Gent, M.R.A. van (1992): Numerical model for wave action on and in coastal structures. *Communications on Hydraulic and Geotechnical Engineering*; Report No. 92-6; Delft University of Technology, Delft.
- Gent, M.R.A. van (1993): Stationary and oscillatory flow through coarse porous media. Faculty of Civil Engineering; *Communications on Hydraulic and Geotechnical Engineering*; Report No. 93-9; pp. 61; Delft University of Technology, Delft.
- Groot, M.B. de; Yamazaki, H.; van Gent, M.R.A.; Kheyruri, Z. (1994): Pore pressures in rubble mound breakwaters. ASCE; *Proceedings International Conference Coastal Engineering (ICCE)*; Vol. 24, No. 2, pp. 1727-1738; Kobe, Japan.
- Gu, Z.; Wang, H. (1991): Gravity waves over porous bottoms. *Coastal Engineering*; Vol. 15, pp. 695-524; Elsevier Science Publishers B.V., Amsterdam.
- Hall, K.R. (1991): Trends in phreatic surface motion in rubble-mound breakwaters. ASCE; *Journal of Waterway, Port, Coastal, and Ocean Engineering*; Vol. 117, No. 2, pp. 179-187; New York;
- Hall, K.R. (1994): Hydrodynamic pressure changes in rubble mound breakwater armour layers. IAHR; *Proceedings International Symposium: Waves - Physical and Numerical Modelling*; pp. 1394-1403; Vancouver, Canada.
- Hannoura, A.A.; Barends, F.B.J. (1981): Non-darcy flow: A state of the art. *Proceedings of Euromech 143*; pp. 37-51; Delft.
- Hannoura, A.A.; McCorquodale, J.A. (1985): Rubble mounds: Hydraulic conductivity equation. ASCE; *Journal of Waterway, Port, Coastal and Ocean Engineering*; Vol. 111, No. 5, pp. 783-799; New York.
- Koenders, M.A. (1985): Hydraulic criteria for filters. Delft Geotechnics, unnumbered Report; Estuary Filters.
- Kozeny, J. (1927): Ueber kapillare Leitung des Wassers im Boden. *Sitzungs-Berichte der Wiener Akademie der Wissenschaft*; Rep. 11a; pp. 271-306; Wien.
- Madsen, O.S. (1974): Wave transmission through porous structures. ASCE; *Journal of Waterways, Harbors and Coastal Engineering Division*; Vol. 100, No. 3, pp. 169-188.
- Muttray, M.; Oumeraci, H.; Zimmermann, C.; Partensky, H.-W. (1992): Wave energy dissipation on and in rubble mound breakwaters. ASCE; *Proceedings International Conference Coastal Engineering (ICCE)*; Vol. 23, pp. 1434-1447; Venice, Italy.
- Muttray, M.; Oumeraci, H.; Zimmermann, C. (1995): Wave-induced flow in a rubble mound breakwater. *Proceedings of Coastal and Port Engineering in Developing Countries*; Vol. 4, pp. 1219-1231; Rio de Janeiro, Brazil.
- Muttray, M. (2000): Wellenbewegung an und in einem geschütteten Wellenbrecher — Laborexperimente im Grossmassstab und theoretische Untersuchungen. *Ph.D. Thesis; Techn. University Braunschweig; Dept. of Civil Engineering*; pp. 282; Germany.
- Oumeraci, H.; Partensky, H.W. (1990): Wave-induced pore pressure in rubble mound breakwater. ASCE; *Proceedings International Conference Coastal*

- Engineering (ICCE)*; Vol. 22, pp. 14; Delft, Netherlands.
- Polubarinova-Kochina, P.Y. (1962): Theory of groundwater movement. Princeton University Press; Princeton, N.J.
- Shih, R.W.K. (1990): Permeability characteristics of rubble material - new formulae. ASCE; *Proceedings International Conference Coastal Engineering (ICCE)*; Vol. 22, No. 2, pp. 1499–1512; Delft, Netherlands.
- Sollit, C.K.; Cross, R.H. (1972): Wave transmission through permeable breakwaters. ASCE; *Proceedings International Conference Coastal Engineering (ICCE)*; Vol. 13, pp. 1827–1846.
- Troch, P.; de Somer, M.; de Rouck, J.; van Damme, L.; Vermeir, D.; Martens, J.P., van Hove, C. (1996): Full scale measurements of wave attenuation inside a rubble mound breakwater. ASCE; *Proceedings International Conference Coastal Engineering (ICCE)*; Vol. 25, No. 2, pp. 1916–1929; Orlando, Florida.
- Troch, P.; de Rouck, J.; van Damme, L. (1998): Instrumentation and prototype measurements at the Zeebrugge rubble mound breakwater. *Coastal Engineering*; Vol. 35, No. 1/2, pp. 141–166; Elsevier Science Publishers B.V., Amsterdam.
- Troch, P. (2001): Experimental study and numerical modelling of pore pressure attenuation inside a rubble mound breakwater. *PIANC Bulletin*; No. 108, pp. 5–27.
- Troch, P.; de Rouck, J.; Burcharth, H.F. (2002): Experimental study and numerical modelling of wave induced pore pressure attenuation inside a rubble mound breakwater. ASCE; *Proceedings International Conference Coastal Engineering (ICCE)*; Vol. 28, No. 2, pp. 1607–1619; Cardiff, Wales.